Kinematic Dissection of Arm Paresis after Focal New M1, Old M1 and Red Nucleus Lesions in Non-Human Primates

Anna Baines[1], Annie Poll[1], Anne M.E. Baker[1], John W. Krakauer[2], Stuart N. Baker[1]

1: Faculty of Medical Sciences, Newcastle University, Newcastle upon Tyne, NE2 4HH, UK.

2: Department of Neurology and Neurosciences, Johns Hopkins University, Baltimore, MD, USA.

Corresponding Author:

Prof. Stuart Baker,

Henry Wellcome Building,

Faculty of Medical Sciences,

Newcastle upon Tyne,

NE2 4HH,

UK.

Email: stuart.baker@ncl.ac.uk

Abstract

Stroke survivors typically transition through a stereotyped sequence of upper limb recovery. After initial weakness and loss of dexterity, spasticity and fixed muscle coactivation patterns (synergies) appear. Early work suggested that different features arise from distinct primary motor cortex (M1) subdivisions. Here we investigated this with modern methods, using focal ischemic lesions of cortex and electrocoagulation lesions of magnocellular red nucleus (RNm) in rhesus monkeys.

Nine animals were trained on a reach and grasp task; hand kinematics were assessed with markerless tracking. Focal M1 lesions within the central sulcus (New M1 in Strick's terminology) and the posterior part of M1 on the gyrus (Posterior Old M1) both produced increases in reach trajectory variability and reductions in speed. The speed deficit was more long-lasting for Posterior Old M1, the trajectory variability deficit was more consistent for New M1. Anterior Old M1 lesions produced only small effects on speed. An extensive cortical lesion, which combined New and Old M1 with pre-motor and somatosensory cortex damage produced no more extensive deficits than lesions to OldM1 or NewM1 alone, suggesting that effects arose mainly from damage to descending pathways rather than cortico-cortical interactions.

Lesions of RNm led to long-lasting slowing of reach, but no increase in variability. Subsequent cortical lesions to Old M1 led to more severe effects, and worse recovery, than without the preceding RNm lesion. This emphasizes a key compensatory role of the rubrospinal tract following cortical damage in monkey, which is not possible in humans where the rubrospinal tract is vestigial.

None of the lesions investigated led to overt abnormal synergies.

The results fit with differences in descending connections from each area: New M1 has fast cortico-motoneuronal output, known to be important for fine motor control (here assessed by trajectory variability); Old M1 has cortico-reticular connections able to activate the reticulospinal tract, important for generating the high forces needed for fast movements.

Introduction

After a stroke, damage to the primary motor cortex (M1) and its descending corticofugal projections results in contralateral hemiparesis. This is seen in more than 80% of patients acutely and 40% chronically (Cramer et al., 1997), as most strokes occur in middle cerebral artery (MCA) territory (Shelton and Reding, 2001). Twitchell (1951) and Brunnstrom (1970) described that upper limb recovery after such strokes typically 'occurs in an almost standardized fashion' (Brunnstrom, 1966). Initial weakness and loss of dexterity (negative signs) are replaced with involuntary increases in muscle activity (positive signs). Heightened reflex responses emerge into poorly coordinated movements dominated by highly stereotyped muscle coactivation patterns or 'synergies'. Abnormal synergies usually eventually disappear, making isolated joint movements possible again. However, it was emphasized that recovery can stall at any one of these stages (Brunnstrom, 1970; Twitchell, 1951), leaving moderate to severe patients with movement repertoires confined to synergies (Beer et al., 2007; Dewald and Beer, 2001; Dewald et al., 1995; Ellis et al., 2007). In patients with the abnormal flexor synergy, shoulder abduction drives simultaneous activation of elbow, wrist and finger flexors, limiting elbow extension (Avni et al., 2024; Lan et al., 2017; Miller and Dewald, 2012; Sukal et al., 2007). MCA strokes are variable, with infarcts often damaging multiple cortical areas in tandem. This prevents assignment of different features of the hemiparetic phenotype (i.e. weakness, loss of dexterity, spasticity, synergies) to specific brain regions. Focal surgical lesions in an animal model paired with careful observation of behavioral effects could provide fundamental knowledge linking anatomy to component deficits. This could allow rational stroke therapies, targeting different treatments for each area damaged.

Studies performed in monkey over 80 years ago showed that positive motor signs did not result from pyramidal tract lesions (Tower, 1940), but were seen after lesions to M1 (Hines, 1937; 1943). Hines noted that positive signs were strongest after damage to a strip approximately 3mm wide located just posterior to Brodmann's area 6 (premotor cortex). Hines reported that this subregion, which she referred to as 'Area 4s', primarily suppresses motor output when stimulated; this was in contrast to mainly excitatory effects from stimulating more posterior M1. Suppressive effects from Area 4s may be mediated by corticobulbar connections (McCulloch et al., 1946) to a region of the reticular formation which suppresses motor output (Du Beau et al., 2012; Engberg et al., 1968; Jankowska et al., 1968; Magoun and Rhines, 1946; Takakusaki et al., 2001). The Area 4s designation has fallen out of current usage, although a modern study which mapped output effects from the lateral motor areas using microstimulation did show a clear band of mainly suppressive effects in the most anterior portion of M1 in one out of the two monkeys examined (Boudrias et al., 2010).

A different approach to subdividing M1 was taken by Rathelot and Strick (2009), who mapped the distribution of cortico-motoneuronal (CM) cells. They reported that CM cells were mainly found in the bank of the central sulcus, not on the gyrus, and coined the terms 'New M1' and 'Old M1' to refer to these two regions. Both parts of M1 have a similar density of corticospinal neurons (Dum and Strick, 1991; He et al., 1993); only Old M1 connects to the brainstem (Keizer and Kuypers, 1989). New M1 is found only in Old World monkeys and humans, and is considered essential for performing dexterous upper limb movements (Lemon, 2008; Rathelot and Strick, 2009). Witham et al. (2016) provided evidence that Old M1 also has CM cells (as was already clear from the work of Rathelot and Strick (2009)) but that these have more slowly conducting axons than those in New M1. Area 4s of Hines would occupy approximately the anterior half of Old M1 as described by Rathelot and Strick.

Given this extensive anatomical and physiological evidence, we hypothesized that focal lesions to the different M1 subregions would lead to distinct post-lesion phenotypes. However, post-lesion deficits are a composite not only of the function that has been lost, but also of the nervous system's ability to

recover and restore that function. Following mild stroke, spared parts of M1 underlie functional recovery (Nudo and Milliken, 1996; Nudo et al., 1996; Rouiller et al., 1998). After larger M1 lesions, ipsilesional motor regions such as the dorsal premotor cortex (PMd) and the supplementary area (SMA) can be recruited to replace lost corticospinal output (Fridman et al., 2004; Johansen-Berg et al., 2002; Liu and Rouiller, 1999; McNeal et al., 2010). In even larger strokes where these areas are also damaged, there is an increased reliance on the contralesional motor cortex to restore connections to the affected side via the cortico-reticulospinal pathway (Zaaimi et al., 2012; Zaaimi et al., 2018). This compensation partially restores upper limb reaching, albeit with poorer quality movements (Choudhury et al., 2025; McPherson et al., 2018).

Charles Sherrington once said, *'…the pyramidal tract is such a human feature… in macaque the recovery is surprising, when contrasted with the degree and persistence of the human condition, which is often permanent, is it not?'* (Walshe, 1961). The marked difference in speed and quality of recovery between macaques and humans after a cortical lesion remains an enigma. One possible explanation could come from differences in the rubrospinal pathway. In humans, the magnocellular red nucleus (RNm) outputs to the spinal cord are notably weak, reflecting an evolutionary shift towards greater cortical control of movement (Herculano-Houzel et al., 2016; Nathan and Smith, 1955; Onodera and Hicks, 2010). By contrast, in monkey the rubrospinal tract is an important motor pathway (Cheney, 1980; Holstege et al., 1988; Mewes and Cheney, 1991; Ralston et al., 1988; Riddle et al., 2009), and is known to be involved in functional recovery (Belhaj-Saïf and Cheney, 2000). It is plausible that without a functional rubrospinal system, monkeys would exhibit similarly limited upper limb recovery as seen in humans; however, this remains unconfirmed.

In this study, we set out to test if focal lesions to the distinct motor cortical subareas described above would result in different deficits. We measured movement speed and trajectory variability, considering them the analogues for reaching of weakness and dexterity in hand function (Cortes et al., 2017; Hadjiosif et al., 2021). We also examined whether recovery was worsened by prior unilateral lesions to RNm, or by extending the cortical lesion size. We show increases in both movement variability and speed after both New M1 and Posterior Old M1 lesions; movement slowing was long-lasting only after Posterior Old M1 lesions. Lesions of Anterior Old M1 (equivalent to Area 4s) had minimal effects. RNm lesions slowed movement only a little, but recovery from a cortical lesion after a preceding RNm lesion was markedly impaired. None of the focal lesions which we tested generated overt positive signs.

Materials and Methods

Experiments were conducted in one male (weight at start of study = 11.1 kg) and eight female rhesus macaques (weights at start of study = 5.5-7.7 kg), referenced in this report as Monkey D, B, Ca, Ch, Cm, Co, Cu, Ca, Ze, and Zd respectively. All animal procedures were carried out under an appropriate license issued by the UK Home Office under the Animals (Scientific Procedures) Act 1986 and were approved by the Animal Welfare and Ethical Review Board of Newcastle University.

Behavioral Task

Animals were trained to perform a reach and grasp task with their right upper limb (Fig. 1A). The neck and left limb were gently restrained throughout. A trial of the task was initiated by the monkey holding a handle for one second. The lid of a baited cup then rapidly retracted, providing access to a food reward contained within. The monkey then made a rapid reaching movement to retrieve the reward. The trainer pressed a foot switch to signal the successful end of the trial. A timeout tone sounded if the footswitch was not pressed within 5 s of handle release; the trial then had to be repeated from

the start. Five or ten repeat trials were performed reaching in the same direction, after which the handle and cup were moved to another of the 12 possible arrangements on the vertices of a diamond (Fig. 1B). This allowed for performance of an assortment of flexion and extension reaches each day.

Most monkeys learnt this task rapidly (3-6 months), and performed it reliably on each session. Three monkeys (Monkey Ze, B and Cm) were consistently given oral trazodone to improve focus and task performance (25-62.5 mg daily dose given 1 hour before training).

Video Recording and Markerless Tracking

Baseline data were collected 5 days per week for 2-5 weeks to sample normal reaching behavior, before the lesion was made. Further kinematic data was then gathered for 15 weeks.

High-speed video footage was recorded from a camera positioned above the monkey (90-100 fps; 1280x1024 resolution; CM3-U3-31S4C-CS 1/1.8" Chameleon®3 Color Camera, Teledyne FLIR, Oregon, USA). Frame capture was driven by regular digital pulses to the camera; these pulses also triggered an 8 bit binary counter, which was connected to 8 LEDs visible within the camera frame. On occasion, the camera software missed writing a frame to disk. We identified such missed frames using a custom MATLAB script which extracted and thresholded the light intensities around each LED to determine the binary count and detect non-contiguous frames. Videos and task parameters were stored to disk.

Videos were processed offline using the open source markerless tracking software DeepLabCut (DLC, version 2.2, (Nath et al., 2019)). A ResNet-50 model pre-trained on an ImageNet database was custom-trained on task video footage to predict right hand location accurately in each video frame. Initial training frames were extracted using a k-means algorithm, and positions of the handle, cup and right index finger metacarpophalangeal joint were manually labelled in each frame. The network was iteratively trained, and prediction accuracy of the three landmarks was reviewed using test video footage (i.e. frames not used for network training). Any further network training was carried out using additional frames manually chosen from poorer tracking scenarios. 3640 frames from sessions with different animals were used for training in total. The error of different iterations of the trained network used for task video analysis was 2-2.6 mm, testing error 2.4-9.5 mm (measured with 0.6 prediction likelihood cutoff).

Hand position and speed over time were low pass-filtered and plotted using custom-written MATLAB scripts. A trial was included in subsequent analyses if it met the following criteria: 1) hand speed exceeded 0.1 m/s within a 200 ms-long window before handle release (reach start) and returned below 0.1 m/s within 400 ms after handle release (reach end); and 2) no more than 4 consecutive missed frames from the camera during this sampling window. For trials that met these criteria and had 1-4 missed frames, missed marker locations were added by interpolation. Maximum speed was extracted over the window between reach start and end. Mahalanobis distance squared (MD^2) analysis was applied to normalized hand location datasets to quantify trajectory variability (Cortes *et al.*, 2017; Hadjiosif *et al.*, 2021). For each trial, trajectories were first normalized to 50 equally-spaced datapoints between reach start and end. MD^2 was calculated for x and y time series with respect to all baseline trials of the same movement direction, and averaged per trial (AMD^2). Median AMD^2 was calculated over each week.

Maximum speed and AMD^2 were averaged over all movement directions, to appreciate overall changes. We also we found the difference between maximum speed and AMD^2 between trials involving elbow flexion *vs* elbow extension; this allowed us to check for relative differences depending

on movement type. For this difference analysis, the standard error of the median per week was estimated using bootstrapping with 1000 iterations. Significant changes in maximum reaching speed and median MD^2 each week compared to the averaged baseline value for each monkey were identified using the two-sample t-test. Significance for both maximum speed and AMD^2 calculations was corrected for multiple comparisons using a Benjamini-Hochberg correction with a false discovery rate of 5%.

Magnocellular Red Nucleus Lesions

All lesion surgeries described in this report were conducted under general anesthesia managed by a veterinary surgeon. Monkeys were initially sedated with an intramuscular injection of ketamine (2-10 mg/kg), medetomidine (3 µg/kg) and midazolam (0.3 mg/kg). During surgical preparation, anesthesia was maintained with sevoflurane inhalation (2-3%). Animals were intubated and ventilated with positive pressure ventilation. A continuous infusion of alfentanil (24-108 µg/kg/hr), ketamine (6 mg/kg/hr), midazolam (0.3 mg/kg/hr), methylprednisolone (5.4 mg/kg/hr), and Hartmann's solution (5 ml/kg/hr) ensured adequate anesthesia, analgesia, anti-inflammation and hydration throughout surgery. The animal was kept warm with a temperature-controlled heating blanket, and also a supply of thermostatically-controlled warm air. Vital sign monitoring included pulse oximetry, heart rate, blood pressure, core and peripheral blood temperature, and end tidal CO_2. Anesthetic doses were adjusted as necessary to maintain a stable plane of deep anesthesia.

In two monkeys, unilateral RNm lesions were performed using an electrocoagulation technique. Animals were placed in a stereotaxic frame; coordinates in the following are given relative to inter-aural line at the midline in anterio-posterior (AP), mediolateral (ML) and dorso-ventral (DV) directions. A craniotomy was made on the left side stretching from AP 2-12A and ML 3.5-6.5 (Belhaj-Saïf et al., 1998; Martin and Bowden, 1996). We began by mapping the oculomotor nuclei, as these are close to RNm and produce easily-visible eye movements upon stimulation. A stainless-steel electrode (MS501G, Micro-Probe, San Jose, US) penetrated at a 5° penetration angle, and was initially positioned to target coordinates AP 7.0A ML 0 DV 5.0. A series of penetrations at various heights and AP locations close to these initial coordinates were made, and single pulse stimuli (biphasic, 0.1 ms per phase) were delivered at each site. Where eye movements were elicited, the intensity was reduced to find the threshold. These were noted on graph paper, producing a fine-grained map of the oculomotor nuclei. The electrode was then repositioned to target an initial site 1 mm to the left of the optimal oculomotor nucleus coordinate, and RNm mapping begun.

The RNm should facilitate motoneurons via rubrospinal pathways; however, under general anesthesia motoneuron excitability is reduced, and it can be difficult to elicit overt activity by stimulating weak inputs. To overcome this, we first delivered a train of stimuli (biphasic pulses, 0.1ms per phase, 700-1000 µA intensity, 3 ms inter-stimulus interval) to the pyramidal tract, and checked for responses in electromyogram (EMG) from the right extensor digitorum communis (EDC) muscle. Pyramidal tract stimulation used a chronic electrode implanted in a previous surgery (not otherwise used in the work reported here). The number of stimuli in the train was increased progressively until an EMG response was produced, and was then reduced by one to obtain a just subthreshold stimulus. The mapping electrode was then advanced to various sites surrounding the expected location of RNm, and stimuli given through it following the subthreshold pyramidal tract stimulation (3 ms interval between the last stimulus in the train to the pyramidal tract and the RNm stimulus). We searched for locations where EDC responses were elicited, and determined the threshold intensity of RNm stimulation required

(25 µA-1 mA). These thresholds were plotted on graph paper, as for the oculomotor nuclei. Lesion locations were determined as the lowest threshold sites.

A direct current was passed at each chosen site to produce a lesion (1 mA for 20 s, or 2 mA for 10 s, electrode positive). Monkey Cm had two lesions at the following stereotaxic locations: AP 6.0A, ML 1.0L, DV 16.9 and AP 7.0A, ML 1.0L, DV 18.0. Monkey Ca had three lesions at AP 5.0A, ML 1.0L, DV 14.6; AP 6.0A, 1.0L, DV 14.3 and AP 7.0A, ML 1.0L, DV 13.7. The electrode used for mapping and lesioning was then removed, and the craniotomy sealed. Both animals recovered from anesthesia and returned to their normal cages later that evening. Broad spectrum antibiotics (oral or subcutaneous co-amoxyclav 12.5 mg/kg), analgesics (intramuscular buprenorphine 0.02 mg/kg; oral or intramuscular meloxicam 0.2 mg/kg; oral paracetamol 23 mg/kg) and steroids (intramuscular dexamethasone 0.2-0.5 mg/ml) were administered. Two days later both animals were well enough to return to the laboratory to perform the task. They received a secondary cortical lesion when kinematic measured plateaued after 7-8 weeks (Monkey Cm – Anterior Old M1; Monkey Ca – Entire Old M1).

Cortical Lesions

Monkeys were placed in a stereotaxic frame under general anesthesia and a craniotomy made on the left side above M1 (approximately 6-20 mm lateral to midline). This lesion laterality was chosen to cover much of the right upper limb representation (8-19 mm) (Boudrias *et al.*, 2010). The anteroposterior extent varied depending on the animal and the intended lesion.

To make lesions of different M1 subregions at the precentral gyrus (i.e. Old M1), the dura was opened to allow for smooth needle penetration. A manipulator was configured with four needles oriented anteroposterior, spaced 1 mm apart, and pre-filled with 900 µM endothelin-1 in saline (HB3442, Hello Bio, Bristol, UK). Endothelin-based models for generating focal ischemic cortical lesions have already been performed effectively in macaques (Herbert et al., 2015a; Herbert et al., 2015b), chosen for its fast-acting and potent vasoconstrictive effects. We anticipated a diffusion radius of approximately 0.5 mm relative to the needle tip. Anteroposterior positioning of needles relative to the central sulcus (CS) determined which lesion was performed (Posterior Old M1 1-4 mm anterior, blue in Fig. 2A; Anterior Old M1 4-7 mm anterior, purple in Fig. 2A). Starting 8mm lateral from the midline, needles first penetrated 2 mm below the surface and were then retracted to 1.3 mm below the surface; this allowed for some tissue dimpling on penetration. Endothelin-1 was infused over two minutes (1 µl per site, 500 nl/min) with needles left in the tissue for a further minute to allow sufficient diffusion. Needles were then moved to the next site 1 mm more lateral. The injections were repeated identically at least 1 hour later to increase the duration of ischemia (Herbert *et al.*, 2015a). In one animal (Monkey Ca), a larger lesion was performed 7 weeks after the RNm lesion. The same method was used but with an increased number of anteroposterior infusion sites (Entire Old M1, 1-7 mm anterior relative to the CS).

To perform deeper lesions of the grey matter in the anterior bank of the CS (New M1), we first used electrophysiological mapping to determine the angle of the CS. A parylene-insulated stainless steel microelectrode (WE30031.0A3, MicroProbe, San Jose, USA) was zeroed mediolaterally to stereotaxic midline and anteroposteriorly to the CS. A ground wire was connected to a needle placed in the skin. The electrode penetrated into the cortex, and single unit recordings were made, noting whether cells were discharging at depths of 0.5-10 mm below the surface. This was repeated for anteroposterior sites 0.5-4 mm anterior to the CS, and at 9.5, 13.5 and 17.5 lateral to midline. The anteroposterior sites

at each laterality that had the largest and most consistent cell firing were used as lesion targets, as these were likely to be within cortical layer V. A four-needle array was configured in a manipulator with 1 mm spacing and oriented approximately mediolaterally, with the angle adjusted to ensure the needles were parallel to the CS. The needles were penetrated to 6.7 mm below surface before being retracted 0.7 mm to allow for tissue dimpling. Endothelin-1 was infused at each site as above. The needles were moved 1 mm higher, and the infusion process repeated to cover 3-6 mm below cortical surface (orange in Fig. 2A). Three such penetrations were made at different medio-lateral locations to cover 8-19 mm from the midline.

At the end of these lesion surgeries, the dura was sutured and craniotomy sealed using Gelfoam (Pfizer, Kent, UK) and dental acrylic (Kemdent, Swindon, UK). Animals recovered in a padded cage under supervision. They received a full program of postoperative care (oral/subcutaneous co-amoxyclav 12.5 mg/kg or oral doxycycline 8 mg/kg; oral/intramuscular meloxicam 0.2 mg/kg; oral paracetamol 23 mg/kg; intramuscular dexamethasone 0.2 mg/ml). All monkeys were well enough to return to their home cages the morning after and returned to the laboratory for recording 2 days post-lesion.

We performed a more extensive cortical lesion in one animal (Monkey D), targeting PMd, Entire M1 and S1 (Brodmann's Areas 1, 2 and 3). This used a combination of the superficial and deep lesioning approaches described above, split into three surgeries each separated by one week. The first surgery entailed mapping both anterior and posterior banks of the CS (New M1 and S1 Brodmann's Area 3a/b, respectively). A craniotomy was made extending 13 mm anterior and 9 mm posterior relative to the CS to cover the final desired lesion extent. The dura was left intact. Maps of cell discharge were compiled from 3 mm anterior to 1 mm posterior relative to the CS, at 9, 12, 15 and 18 mm lateral to the midline, and between 1-12 mm below the cortical surface. The craniotomy was then sealed as above.

One week later, the dental acrylic over the craniotomy was removed, and a surgery to produce deep lesions of anterior and posterior banks of the CS was carried out. Two manipulators holding either a four or six-needle array were pre-filled with endothelin-1 and oriented antero-posteriorly with 1 mm spacing. The most posterior needle of each array was zeroed to midline. The four needle array sites were penetrated in turn from 8-13 mm lateral, the six needle array from 14-19 mm lateral. At each laterality in turn, the needles penetrated to an appropriate depth and anteroposterior location relative to CS as determined from mapping to cover both pre- and post-central sulcus. Endothelin-1 infusions were made over 1.5 minutes (1 µl per site, 667 nl/min). Needles were left in place for a further minute before being moved to the next site 1 mm higher. When all depths were lesioned (i.e. from initial infusion depth to 2 mm below surface, pink in Fig. 2B), the needle arrays were withdrawn, moved 1 mm more lateral, and the protocol repeated. All lesions were repeated after approximately one hour as described above. At the end of surgery, the craniotomy was sealed and appropriate post-operative care given (both as previously described). Monkey D was well enough to return to the laboratory and the task two days after this first lesion.

A final surgery to lesion superficial cortical regions both anterior and posterior to the CS (PMd, Old M1, S1 Brodmann's Areas 1 and 2) was performed one week later. The protocol used was similar to that previously described for lesions of Old M1, except that two needle arrays with four or six needles oriented antero-posteriorly were used simultaneously to cover a larger anteroposterior extent (green in Fig. 2B). In a first set of injections, the six needle array covered 1-6 mm anterior to CS, and the four needle array 1-4 mm posterior to CS. These injections were repeated after one hour. In the second set,

injections covered 7-12 mm anterior and 5-8 mm posterior to CS, respectively; these were also repeated after one hour. At the end of the surgery the dura was repaired, the craniotomy sealed, and appropriate post-operative therapy given (as preciously described). Laboratory recording restarted two days after this second lesion.

At 15 weeks post-lesion, animals were terminally anesthetized with an overdose of propofol and perfused through the heart with phosphate buffered saline followed by formalin for fixation of tissues. For the remainder of this report we will refer to lesions by their target locations; detailed confirmation of exact lesion extents has not yet been confirmed with histology.

Results

Impact of Cortical Lesions on Reaching Performance

None of the lesions reported here resulted in a clinical presentation resembling the flexor synergy seen in human stroke survivors—that is, elbow flexion occurring in conjunction with shoulder abduction. Application of sensitive quantitative measures capable of detecting flexor synergy in a subset of these animals will be discussed in a future publication. In this report, we focus on differences in negative motor phenotypes.

Figure 3 shows example kinematic measurements before and after a lesion. In Fig. 3A, reach trajectories are shown for each of the 12 possible movements, from the handle starting position (white square) to the cup (three locations shown in red, green and black on each plot). Trajectories post-lesion were clearly more variable. Figure 3B illustrates the instantaneous speed plots for a single movement direction. The left trace shows raw data, with an x-axis in seconds; each movement lasts a slightly different time. The right trace shows traces normalized in length between movement onset and offset; data processed in this way were used for the AMD^2 analysis. Movements after the lesion were a little slower, more variable, and in some cases had pronounced two components.

Figure 4 presents changes to two kinematic assessments pre- and post-lesion for each monkey: AMD^2 (red) and maximum speed (blue). These measures were averaged over all reaching directions to assess overall reaching performance regardless of any differences in reaches requiring flexion or extension. AMD^2 provides a quantitative measure of trajectory variability. Increased AMD^2 scores reflect a reduced ability to control muscles independently which is required for accurate straight line reaching movements, and may thus be a proximal analogue of lowered dexterity in the hand. Reduced maximum speed by contrast may indicate weakness. In all monkeys scores after the lesion were compared with the pre-lesion baseline. Most recovery occurred 1-4 weeks post-lesion (the spontaneous recovery period), similar to the recovery window previously described in humans (Cortes *et al.*, 2017). Recovery usually plateaued within ~8 weeks.

Comparing cortical lesions in different divisions of M1 (New M1 vs Posterior Old M1 vs Anterior Old M1) showed different recovery outcomes. Lesions to both New M1 and Posterior Old M1 had significant impacts on trajectory variability, which remained permanently higher than baseline in all four animals. Lesions to these two regions also produced significant slowing of maximum reaching speed; however, this was more sustained after Posterior Old M1 lesions, with a permanent slowing. Previous work has shown that Posterior Old M1 has mixed outputs via both corticospinal and corticoreticulospinal tracts (Keizer and Kuypers, 1989), and that the majority of drive to motoneurons producing movement in primates comes from the reticulospinal tract (Tapia et al., 2022). We suggest that without strong and coordinated facilitation of motoneurons via the cortico-reticulospinal tract,

permanently slower movements resulted after Posterior Old M1 lesions. Conversely, Anterior Old M1 lesions led to minimal effects on AMD^2. Maximum speed was reduced in one animal only for the immediate week post-lesion; for the other, the effect was greater, but recovery was complete by the end of the recorded period. These results suggested that New M1 and Posterior Old M1 areas have strongly facilitatory effects on the upper limb, whereas Anterior Old M1 plays a distinctly different role.

In Monkey D, we tested the effect of a very large cortical lesion (PMd, M1, S1 Brodmann's Areas 1, 2 and 3). Surprisingly, the effects were not as severe as anticipated for a grey matter lesion of this magnitude (for the upper limb representations, only SMA was left intact on the ipsilesional side). Following New M1 and S1 Brodmann's Area 3a/3b lesions (lesion surgery 1, first solid vertical line in Fig. 4), there was a large increase in AMD^2 score, but no change in maximum speed. Subsequent lesions to PMd, Old M1 and Broadman's Areas 1 and 2 (lesion surgery 2) had the opposite effect, with decreased speed but no further negative impact on AMD^2. Both metrics remained significantly worse than baseline by 15 weeks post-lesion.

Interestingly, no additional deficits in quality of reaching (AMD^2) were observed in Monkey D following combined lesions to S1 Brodmann's Areas 3a/3b and New M1, compared to lesions to New M1 alone (Monkeys Ze and Cu). A similar pattern was noted in the same animal regarding reach speed, with no further reduction observed after combined lesions to PMd, S1 Brodmann's Areas 1 and 2, and Old M1, relative to Old M1 lesions alone (Monkeys B and Co). These findings suggest that additional damage to somatosensory or premotor areas did not exacerbate reach impairment beyond that caused by M1 injury alone.

Impact of RNm followed by Cortical Lesions on Overall Reaching Performance

Two animals underwent lesions of RNm, with consistent effects (region between dotted and solid vertical lines in Fig. 4). In both there were significant and persistent reductions in speed (but not AMD^2), however these were smaller in amplitude compared to New M1/Posterior Old M1 lesions.

Comparing data from Monkey Cm (RNm plus Anterior Old M1 lesion) and Monkeys Zd and Ch (identical cortical lesion without prior RNm lesion) provided insights into the contribution of the rubrospinal tract to recovery following cortical injury. The Anterior Old M1 lesion had greater effects on AMD^2 and speed after the preceding RNm lesion than when the cortical lesion occurred against the background of a healthy rubrospinal outputs. The deficits persisted until the end of the recorded period.

In Monkey Cd, an entire Old M1 lesion after the preceding RNm lesion led to the poorest recovery seen in our study, with large deficits in both speed and AMD^2 which improved little. Notably, this animal was more severely affected than Monkey D, which had a much larger cortical lesion. These results therefore serve to highlight further the importance of RNm as a route for recovery in monkey.

Overall, the results from RNm lesions suggest a role for the rubrospinal system in generating fast reaches, and in contributing to recovery after cortical damage. Also, the data further emphasize the detrimental consequences of losing Posterior Old M1 in addition to Anterior Old M1, as this is the only difference separating Monkey Cm (RNm plus Anterior Old M1, better overall recovery) and Monkey Cd (RNm plus entire Old M1, much poorer recovery).

Impact of Cortical Lesions to Flexion vs Extension Reaching Performance

Imbalanced recovery is a common finding in stroke survivors, who are often left with overactive flexors and weak extensors (Kamper et al., 2003). Figure 5 examines whether there was a difference in impairment between movements which required elbow flexion or extension, by plotting differences between AMD^2 and maximum speed for flexion vs extension.

Monkeys with New M1 and Posterior Old M1 lesions showed poorer extension reaching performance. This was most evident in Monkey Ze (New M1), where the speed deficit of extension reaches was persistently greater than for flexion. Greater deficits in AMD^2 for extension were also seen in all four animals, although the magnitude and persistence of this difference varied.

Anterior Old M1 lesions caused minimal effects to either kinematic measure (Fig. 4), and there were accordingly small or non-existent flexor-extensor differences observed (Fig. 5).

In Monkey D, the initial lesion of New M1 and Brodmann's Area 3 produced greater slowing and higher trajectory variability for flexion than extension. The second lesion which encompassed PMd, Old M1 and Brodmann's Area 1 and 2 increased this flexion-extension difference in AMD^2.

Impact of RNm and Cortical Lesions to Flexion vs Extension Reaching Performance

After RNm lesions alone (dotted vertical line in Fig. 5), monkeys showed more significant slowing of flexion reaches. There was generally no trend towards worse AMD^2 in a particular direction in either animal following this lesion. However, the greater reduction in speed with flexion became exacerbated in both monkeys after cortical lesions. This is a surprising result, as it is the opposite of the slower extension seen after cortical lesion alone. Flexion-extension differences in AMD^2 after cortical damage were inconsistent, with a brief period of worse extension for Monkey Cm with the smaller cortical lesion, but a larger and more slowly recovering difference towards worse flexion for Monkey Ca. In both animals, reaching speed showed a consistent and long-lasting difference, with slower flexion than extension. To summarize, RNm and cortical lesions combined appeared to show converse, larger and (at least for speed) longer-lasting flexion-extension differences compared to monkeys with normal rubrospinal outputs.

Discussion

Relative Differences in Negative Motor Phenotypes Following Focal Cortical Lesions

Posterior Old and New M1 lesions both produced subtle deficits upon observation of the animals, but these were nevertheless clear in kinematic metrics. Tabel 1 provides a summary of our findings. Both areas have significant corticospinal outputs (Dum and Strick, 1991; He *et al.*, 1993; Keizer and Kuypers, 1989) and CM cell populations (Rathelot and Strick, 2009; Witham *et al.*, 2016), which provide important inputs to upper limb motoneurons in healthy animals. When deprived of these contributions animals were weak (slowed movements), clarifying the primary facilitatory roles of these parts of M1. Posterior Old M1 additionally has many cortico-reticulospinal outputs (Fisher et al., 2021; Keizer and Kuypers, 1989), unlike New M1. It has been proposed that most drive to motoneurons during a voluntary movement comes from reticulospinal (not corticospinal) neurons (Tapia *et al.*, 2022). It seems probable that Posterior Old M1 lesions led to a greater reduction in input to motoneurons than New M1 lesions. This could explain the lasting speed deficit in Posterior Old M1 lesioned animals, which was not seen after damage to New M1.

Lesions to New M1 and Posterior Old M1 both had an impact on reaching quality. Fast-conducting CM cells are found in New M1 and Area 3a (Rathelot and Strick, 2006; 2009). There are also some CM cells in Old M1, but these are slower and generate weaker effects on motoneurons (Innocenti et al., 2019; Witham *et al.*, 2016). Kinematics data gathered from Monkey D in particular highlights the differential effects of lesions to different cell populations (Figure 4). Focal lesions to New M1 and S1 Brodmann's Areas 3a/3b negatively affected trajectory variability (but not speed). Subsequent lesions to PMd, Old M1 and S1 Brodmann's Areas 1 and 2 one week later led to no further impairment in trajectory variability but poorer reaching speed. Overall, our results suggest that lesions affecting corticoreticular

outputs (Old M1) contribute more significantly to weakness because of a greater reduction of overall drive to motoneurons. By contrast, deeper lesions of tissue surrounding the central sulcus (New M1) damage fast corticomotoneuronal outputs and impair the quality of motor control. Some impairment of movement quality is also produced by lesions of Posterior Old M1, with its slower CM cell output.

We suggest that effects following lesions in Monkey D were predominately due to loss of M1 regions, rather than somatosensory and premotor areas. Firstly, deleterious effects to reaching dexterity (increases in AMD[2] during acute recovery) were comparable following combined lesions of Areas 3a/3b and New M1 compared to New M1 alone. There are no CM cells in Area 3b; the CM cell population found in Area 3a is suggested to target primarily γ-motoneurons involved in fusimotor control (Rathelot and Strick, 2006; 2009). By contrast, CM cells from New M1 project to α-motoneurons at short latencies (Witham *et al.*, 2016). Our findings imply that trajectory variability may be the proximal analogue of dexterity in the hand, which is known to be most significantly mediated by CM cells (Porter and Lemon, 1993).

Secondly, we observed no further reductions in reaching speed after combined lesions to PMd and Areas 1 and 2 with Old M1 relative to Old M1 lesions alone. This is likely because these areas are predominantly involved in the modulation of M1 output, rather than serving as a primary source of motor commands to α-motoneurons (Dum and Strick, 2005; Widener and Cheney, 1997). This implies that damage to descending pathways, rather than to cortico-cortical connections, is the main determinant of deficits.

Reaching deficits after lesions to Anterior Old M1 were small or absent, even though a similar area of cortex had been targeted as for Posterior Old M1 (Fig. 2). This absence of substantial negative signs supports the idea that the area 4s of Hines (1943) has a different role from other M1 subregions. Previous work supported Hines' idea that it is primarily suppressive (Boudrias *et al.*, 2010; de Barenne and McCulloch, 1941), but we did not find any evidence of disinhibition after Anterior Old M1 lesions. Moderns maps of effects elicited by M1 stimulation show intermixed suppression and facilitation throughout M1 (Boudrias *et al.*, 2010), although suppression is more common for Anterior Old M1. Loss of suppression from Anterior Old M1 could therefore easily by compensated for from other parts of M1. If, as suggested by McCulloch *et al.* (1946), suppression from area 4s is partly exerted via cortico-reticulospinal outputs, there would be even more options for recovery, as the primate reticular formation receives widely converging inputs from M1 and pre-motor regions in both hemispheres (Fisher *et al.*, 2021).

Poorer Recovery with Combined Lesions to RNm and M1 Regions

Non-human primates are a valuable model for translational stroke research (Lin et al., 2023) due to their neuroanatomical and physiological similarities to the human motor system (Bortoff and Strick, 1993; Decramer et al., 2018; Lemon, 2008; Lemon et al., 2002; Mu et al., 2023; Porter, 1987). However, there are clear functional differences in red nucleus outputs between monkeys and humans. RNm cells make an important contribution to upper limb movements in monkeys, particularly those involving the hand (Belhaj-Saïf *et al.*, 1998; Gibson et al., 1985; Mewes and Cheney, 1994; Miller et al., 1993; Van Kan and McCurdy, 2001; Van Kan and McCurdy, 2002a; b). By contrast, the rubrospinal tract is considered vestigial in humans (Basile et al., 2021; Hatschek, 1907; Massion, 1988; Nathan and Smith, 1955; Ten Donkelaar, 1988). With this anatomical background, we hypothesized that RNm lesions combined with lesions to M1 in monkeys would lead to poorer, more human-like recovery.

Our results show that the rubrospinal tract does indeed contribute to recovery of reaching in monkeys following cortical damage. After RNm lesions alone (Figure 4 after dotted vertical line; Monkey Cm and

Ca), reaching movements were significantly slower, likely due to a reduction of rubro-motoneuronal connections that would usually be responsible for facilitating both proximal and distal upper limb muscles (Belhaj-Saïf *et al.*, 1998; Miller *et al.*, 1993). These inputs were irreplaceable by surviving motor areas (ipsilesional M1, supplementary motor area, reticular formation), emphasizing their important contributions to healthy reaching movements. However, trajectory variability remained unaffected, possibly because monosynaptic outputs to motoneurons from M1 remained intact. Despite these selective and modest effects of a RNm lesion alone, when combined with cortical lesions the effects were substantial. Combined lesions to RNm and all of Old M1 led to severe effects, and the poorest recovery in the entire study (Figure 4; Monkey Ca), despite this animal receiving a smaller infarct than Monkey D.

We also report a striking better recovery of elbow extension relative to poorer elbow flexion in both animals with RNm lesions (Figure 5; Monkey Cm and Ca). This is the opposite to what is typically observed in humans after stroke, where recovery of flexor muscles is favored (Baker et al., 2015; Kamper *et al.*, 2003). It is also unexpected given the known preference for rubrospinal outputs to target extensor muscles more strongly (Belhaj-Saïf *et al.*, 1998; Mewes and Cheney, 1991); we might therefore expect RNm lesions to produce selective deficits in extension. However, after unilateral pyramidology rubrospinal neurons show plasticity and begin to cofacilitate motoneurons innervating flexor muscles and extensor muscles, thereby restoring lost corticospinal inputs to flexors (+340% increased facilitation of flexors, -8% for extensors compared to controls, (Belhaj-Saïf and Cheney, 2000)). This compensatory mechanism may have been compromised following RNm lesions in our animals, resulting in imbalanced facilitation of extensor muscles and subsequent poorer flexion reaching ability that never recovered.

Our findings collectively reaffirm that the monkey rubrospinal system is important for restoring input to motoneurons following corticospinal loss, just as has been previously shown in the rat (Ishida et al., 2019). Without functioning rubrospinal outputs, recovery in monkey does become more similar to that in human, where the rubrospinal tract has been replaced through evolution in favor of an increased reliance on the corticospinal tract.

No Overt Flexor Synergy Expression Following Focal Cortical Lesions

One suggestion in the literature is that abnormal synergies result from a loss of fine control signals from M1, increasing reliance on motor areas with an innate preference for coding synergistic co-contractions and insufficient fractionated control of shoulder and elbow muscles (e.g. the contralesional cortico-reticulospinal tract, (McPherson *et al.*, 2018)). Lesions to Anterior Old M1 seemed the most appropriate cortical target for generating abnormal flexor synergy based on previous literature. 'Area 4s' (found in the anterior region of Old M1) seems capable of exerting powerful suppressive influences over spinal cord motoneuron pools via the cortico-reticulospinal pathway in healthy animals (Boudrias *et al.*, 2010; de Barenne and McCulloch, 1941; Du Beau *et al.*, 2012; Engberg *et al.*, 1968; Jankowska *et al.*, 1968; Magoun and Rhines, 1946; Takakusaki *et al.*, 2001). Ablation of Area 4s was previously described to produce exaggerated stretch reflexes, especially in elbow flexors (Hines, 1936; Hines, 1937; 1943).

We initially hypothesized that isolated damage to Anterior Old M1 would cause impaired suppression of subcortical circuits, resulting in an abnormal flexor synergy pattern. This was not the case. Anterior Old M1-lesioned monkeys were able to extend the elbow within days after the surgery and exhibited only minimal disruptions to reaching kinematics. One explanation may lie in the focal nature of the lesions used in this study, which targeted shoulder, elbow, wrist, and partial hand representations - likely preserving sufficient surrounding cortical tissue and descending pathways to support

compensation and prevent overt synergy expression. A similar rationale may apply to the other lesion conditions tested in this study, none of which produced clear synergy patterns. Importantly, all animals retained intact outputs from the supplementary motor area (SMA). Some SMA neurons form monosynaptic connections with spinal motoneurons (Jürgens, 1984); they exhibit significant plasticity following injury, contributing to functional recovery (Liu and Rouiller, 1999; McNeal *et al.*, 2010).

Early studies which reported positive signs from area 4s lesions employed lesion techniques where the targeted grey matter was surgically removed. This may have inadvertently damaged underlying white matter, thereby disrupting corticospinal and subcortical control beyond the intended Area 4s. Such more extensive damage could compromise cortical inhibition of subcortical systems and remove options for compensation, and lead to the emergence of abnormal synergies.

To summarize, it seems that the lack of flexor synergy expression in our animals was due to focal lesions generating insufficient damage to corticospinal fibers. With sufficient surviving ipsilesional cortex, compensatory strategies involving the contralesional cortex (Cao et al., 1998; Ward et al., 2003) or reticular formation (Choudhury *et al.*, 2025; McPherson *et al.*, 2018) were probably unnecessary, and the unwanted side effects from using these pathways were avoided.

Conclusion

This study reveals nuanced differences between the effect of focal M1 lesions. Lesions of New M1 and Posterior Old M1 both produced effects in trajectory variability and movement speed. However, New M1 had a greater effect on trajectory variability (especially when combined with an area 3 lesion), as might be expected given its fast CM connections. By contrast, lesions of Posterior Old M1 produced more long-lasting deficits in speed; this is also expected, given the extensive cortico-reticular output from this area. Effects from lesions of Anterior Old M1 were slight, consistent with the idea that this area plays a distinctively different role in motor control from the other parts of M1, possibly involving suppression. Damage to the RNm alone produced small but persistent effects limited to movement speed, but also markedly accentuated the deficits following subsequent cortical lesions. These results provide new insights into the generation of the mulit-faceted phenotype of post-stroke hemiparesis. They reveal that the effects depend on an interplay between descending anatomy of the region damaged, and the ability of other areas to compensate. Strikingly, the effects of a large lesion which encompassed all of M1, S1 and pre-motor cortex were no worse than those after much more focal lesions. This suggests that many of the consequences of large infarcts often seen from MCA strokes in humans can be understood in terms of component damage to descending pathways, rather than damage to cortico-cortical interactions.

Acknowledgements

The authors wish to thank Andrew Atkinson, Terri Jackson and Stevie O'Keefe for animal training; Norman Charlton for engineering support; Kathy Murphy, Rocio Palacios O'Connor, Fiona Douglas and Ines Sanchez Garcia for veterinary assistance; and Michelle Waddle for surgical theatre nursing.

Funding

This work was supported by NIH grant 5R01NS119319.

References

Avni, I., Arac, A., Binyamin-Netser, R., Kramer, S., Krakauer, J.W., and Shmuelof, L. (2024). The Kinematics of 3D Arm Movements in Sub-Acute Stroke: Impaired Inter-Joint Coordination is Attributable to Both Weakness and Flexor Synergy Intrusion. Neurorehabilitation and neural repair *38*, 646-658.

Baker, S.N., Zaaimi, B., Fisher, K.M., Edgley, S.A., and Soteropoulos, D.S. (2015). Pathways mediating functional recovery. Progress in brain research *218*, 389-412.

Basile, G.A., Quartu, M., Bertino, S., Serra, M.P., Boi, M., Bramanti, A., Anastasi, G.P., Milardi, D., and Cacciola, A. (2021). Red nucleus structure and function: from anatomy to clinical neurosciences. Brain Structure and Function *226*, 69-91.

Beer, R.F., Ellis, M.D., Holubar, B.G., and Dewald, J.P. (2007). Impact of gravity loading on post-stroke reaching and its relationship to weakness. Muscle & Nerve: Official Journal of the American Association of Electrodiagnostic Medicine *36*, 242-250.

Belhaj-Saïf, A., and Cheney, P.D. (2000). Plasticity in the distribution of the red nucleus output to forearm muscles after unilateral lesions of the pyramidal tract. Journal of Neurophysiology *83*, 3147-3153.

Belhaj-Saïf, A., Karrer, J.H., and Cheney, P.D. (1998). Distribution and characteristics of poststimulus effects in proximal and distal forelimb muscles from red nucleus in the monkey. Journal of Neurophysiology *79*, 1777-1789.

Bortoff, G.A., and Strick, P.L. (1993). Corticospinal terminations in two new-world primates: further evidence that corticomotoneuronal connections provide part of the neural substrate for manual dexterity. Journal of Neuroscience *13*, 5105-5118.

Boudrias, M.-H., McPherson, R.L., Frost, S.B., and Cheney, P.D. (2010). Output properties and organization of the forelimb representation of motor areas on the lateral aspect of the hemisphere in rhesus macaques. Cerebral cortex *20*, 169-186.

Brunnstrom, S. (1966). Motor Testing Procedures in Hemiplegia: Based on Sequential Recovery Stages. Physical Therapy *46*, 357-375.

Brunnstrom, S. (1970). Movement Therapy in Hemiplegia: A Neurophysiological Approach (New York, NY: Harper & Row).

Cao, Y., D'olhaberriague, L., Vikingstad, E., Levine, S., and Welch, K. (1998). Pilot study of functional MRI to assess cerebral activation of motor function after poststroke hemiparesis. Stroke *29*, 112-122.

Cheney, P. (1980). Response of rubromotoneuronal cells identified by spike-triggered averaging of EMG activity in awake monkeys. Neuroscience letters *17*, 137-141.

Choudhury, S., Baines, A., Sarkar, S., Bayen, A.B., Sarkar, S., Baker, M.R., Kumar, H., and Baker, S.N. (2025). Association of a kinematic measure of upper limb reaching and StartReact in chronic hemiparetic stroke. Experimental Brain Research *243*, 1-10.

Cortes, J.C., Goldsmith, J., Harran, M.D., Xu, J., Kim, N., Schambra, H.M., Luft, A.R., Celnik, P., Krakauer, J.W., and Kitago, T. (2017). A short and distinct time window for recovery of arm motor control early after stroke revealed with a global measure of trajectory kinematics. Neurorehabilitation and neural repair *31*, 552-560.

Cramer, S.C., Nelles, G., Benson, R.R., Kaplan, J.D., Parker, R.A., Kwong, K.K., Kennedy, D.N., Finklestein, S.P., and Rosen, B.R. (1997). A functional MRI study of subjects recovered from hemiparetic stroke. Stroke *28*, 2518-2527.

de Barenne, J.D., and McCulloch, W. (1941). Suppression of motor response obtained from area 4 by stimulation of area 4s. Journal of Neurophysiology *4*, 311-323.

Decramer, T., Swinnen, S., Van Loon, J., Janssen, P., and Theys, T. (2018). White matter tract anatomy in the rhesus monkey: a fiber dissection study. Brain Structure and Function *223*, 3681-3688.

Dewald, J.P., and Beer, R.F. (2001). Abnormal joint torque patterns in the paretic upper limb of subjects with hemiparesis. Muscle & Nerve: Official Journal of the American Association of Electrodiagnostic Medicine *24*, 273-283.

Dewald, J.P., Pope, P.S., Given, J.D., Buchanan, T.S., and Rymer, W.Z. (1995). Abnormal muscle coactivation patterns during isometric torque generation at the elbow and shoulder in hemiparetic subjects. Brain *118*, 495-510.
Du Beau, A., Shrestha, S.S., Bannatyne, B., Jalicy, S., Linnen, S., and Maxwell, D. (2012). Neurotransmitter phenotypes of descending systems in the rat lumbar spinal cord. Neuroscience *227*, 67-79.
Dum, R.P., and Strick, P.L. (1991). The origin of corticospinal projections from the premotor areas in the frontal lobe. Journal of Neuroscience *11*, 667-689.
Dum, R.P., and Strick, P.L. (2005). Frontal lobe inputs to the digit representations of the motor areas on the lateral surface of the hemisphere. Journal of Neuroscience *25*, 1375-1386.
Ellis, M.D., Acosta, A.M., Yao, J., and Dewald, J.P. (2007). Position-dependent torque coupling and associated muscle activation in the hemiparetic upper extremity. Experimental brain research *176*, 594-602.
Engberg, I., Lundberg, A., and Ryall, R. (1968). Reticulospinal inhibition of transmission in reflex pathways. The Journal of Physiology *194*, 201-223.
Fisher, K.M., Zaaimi, B., Edgley, S.A., and Baker, S.N. (2021). Extensive cortical convergence to primate reticulospinal pathways. Journal of Neuroscience *41*, 1005-1018.
Fridman, E.A., Hanakawa, T., Chung, M., Hummel, F., Leiguarda, R.C., and Cohen, L.G. (2004). Reorganization of the human ipsilesional premotor cortex after stroke. Brain *127*, 747-758.
Gibson, A., Houk, J., and Kohlerman, N. (1985). Relation between red nucleus discharge and movement parameters in trained macaque monkeys. The Journal of Physiology *358*, 551-570.
Hadjiosif, A.M., Branscheidt, M., Anaya, M.A., Runnalls, K.D., Keller, J., Bastian, A.J., Celnik, P.A., and Krakauer, J.W. (2021). Positive and negative stroke signs revisited: dissociations between synergies, weakness, and impaired reaching dexterity. medRxiv, 2021.2007. 2021.21260448.
Hatschek, R. (1907). Zur vergleichenden Anatomie des Nucleus ruber tegmenti. Arbeiten Aus Dem Neurologischen Institute An Der Wiener Universität *15*, 89.
He, S.-Q., Dum, R.P., and Strick, P.L. (1993). Topographic organization of corticospinal projections from the frontal lobe: motor areas on the lateral surface of the hemisphere. Journal of Neuroscience *13*, 952-980.
Herbert, W.J., Powell, K., and Buford, J.A. (2015a). Evidence for a role of the reticulospinal system in recovery of skilled reaching after cortical stroke: initial results from a model of ischemic cortical injury. Experimental brain research *233*, 3231-3251.
Herbert, W.J., Powell, K., and Buford, J.A. (2015b). Evidence for a role of the reticulospinal system in recovery of skilled reaching after cortical stroke: initial results from a model of ischemic cortical injury. Exp Brain Res *233*, 3231-3251. 10.1007/s00221-015-4390-x.
Herculano-Houzel, S., Kaas, J.H., and de Oliveira-Souza, R. (2016). Corticalization of motor control in humans is a consequence of brain scaling in primate evolution. Journal of Comparative Neurology *524*, 448-455.
Hines, M. (1936). The anterior border of the monkey's (Macaca mulatta) motor cortex and the production of spasticity. Am. J. Physiol *116*, 76.
Hines, M. (1937). The "Motor" Cortex. Bulletin of the John Hopkins Hospital *60*, 313-336.
Hines, M. (1943). Control of movement by the cerebral cortex in primates. Biological Reviews *18*, 1-31.
Holstege, G., Blok, B.F., and Ralston, D.D. (1988). Anatomical evidence for red nucleus projections to motoneuronal cell groups in the spinal cord of the monkey. Neuroscience letters *95*, 97-101.
Innocenti, G.M., Caminiti, R., Rouiller, E.M., Knott, G., Dyrby, T.B., Descoteaux, M., and Thiran, J.-P. (2019). Diversity of cortico-descending projections: histological and diffusion MRI characterization in the monkey. Cerebral Cortex *29*, 788-801.
Ishida, A., Kobayashi, K., Ueda, Y., Shimizu, T., Tajiri, N., Isa, T., and Hida, H. (2019). Dynamic Interaction between Cortico-Brainstem Pathways during Training-Induced Recovery in Stroke Model Rats. J Neurosci *39*, 7306-7320. 10.1523/JNEUROSCI.0649-19.2019.

Jankowska, E., Lund, S., Lundberg, A., and Pompeiano, O. (1968). Inhibitory effects evoked through ventral reticulospinal pathways. Archives italiennes de biologie *106*, 124-140.
Johansen-Berg, H., Rushworth, M.F., Bogdanovic, M.D., Kischka, U., Wimalaratna, S., and Matthews, P.M. (2002). The role of ipsilateral premotor cortex in hand movement after stroke. Proceedings of the National Academy of Sciences *99*, 14518-14523.
Jürgens, U. (1984). The efferent and afferent connections of the supplementary motor area. Brain research *300*, 63-81.
Kamper, D., Harvey, R.L., Suresh, S., and Rymer, W.Z. (2003). Relative contributions of neural mechanisms versus muscle mechanics in promoting finger extension deficits following stroke. Muscle & Nerve: Official Journal of the American Association of Electrodiagnostic Medicine *28*, 309-318.
Keizer, K., and Kuypers, H. (1989). Distribution of corticospinal neurons with collaterals to the lower brain stem reticular formation in monkey (Macaca fascicularis). Experimental Brain Research *74*, 311-318.
Lan, Y., Yao, J., and Dewald, J.P. (2017). The impact of shoulder abduction loading on volitional hand opening and grasping in chronic hemiparetic stroke. Neurorehabilitation and neural repair *31*, 521-529.
Lemon, R.N. (2008). Descending pathways in motor control. Annual Review of Neuroscience *31*, 195-218.
Lemon, R.N., Maier, M., Armand, J., Kirkwood, P.A., and Yang, H. (2002). Functional differences in corticospinal projections from macaque primary motor cortex and supplementary motor area. Sensorimotor Control of Movement and Posture, 425-434.
Lin, X., Wang, H., Huang, S., Chen, L., Yang, S., Zhao, P., Lin, Z., Yang, J., Ruan, L., and Ni, H. (2023). A reliable nonhuman primate model of ischemic stroke with reproducible infarct size and long-term sensorimotor deficits. Aging and Disease *14*, 245.
Liu, Y., and Rouiller, E.M. (1999). Mechanisms of recovery of dexterity following unilateral lesion of the sensorimotor cortex in adult monkeys. Experimental brain research *128*, 149-159.
Magoun, H.W., and Rhines, R. (1946). An inhibitory mechanism in the bulbar reticular formation. Journal of neurophysiology *9*, 165-171.
Martin, R.F., and Bowden, D.M. (1996). A stereotaxic template atlas of the macaque brain for digital imaging and quantitative neuroanatomy. Neuroimage *4*, 119-150.
Massion, J. (1988). Red nucleus: past and future. Behavioural brain research *28*, 1-8.
McCulloch, W., Graf, C., and Magoun, H. (1946). A cortico-bulbo-reticular pathway from area 4-s. Journal of Neurophysiology *9*, 127-132.
McNeal, D.W., Darling, W.G., Ge, J., Stilwell-Morecraft, K.S., Solon, K.M., Hynes, S.M., Pizzimenti, M.A., Rotella, D.L., Vanadurongvan, T., and Morecraft, R.J. (2010). Selective long-term reorganization of the corticospinal projection from the supplementary motor cortex following recovery from lateral motor cortex injury. Journal of Comparative Neurology *518*, 586-621.
McPherson, J.G., Chen, A., Ellis, M.D., Yao, J., Heckman, C., and Dewald, J.P. (2018). Progressive recruitment of contralesional cortico-reticulospinal pathways drives motor impairment post stroke. The Journal of physiology *596*, 1211-1225.
Mewes, K., and Cheney, P.D. (1991). Facilitation and suppression of wrist and digit muscles from single rubromotoneuronal cells in the awake monkey. Journal of Neurophysiology *66*, 1965-1977.
Mewes, K., and Cheney, P.D. (1994). Primate rubromotoneuronal cells: parametric relations and contribution to wrist movement. Journal of Neurophysiology *72*, 14-30.
Miller, L., Van Kan, P., Sinkjaer, T., Andersen, T., Harris, G., and Houk, J. (1993). Correlation of primate red nucleus discharge with muscle activity during free-form arm movements. The Journal of physiology *469*, 213-243.
Miller, L.C., and Dewald, J.P. (2012). Involuntary paretic wrist/finger flexion forces and EMG increase with shoulder abduction load in individuals with chronic stroke. Clinical neurophysiology *123*, 1216-1225.

Mu, J., Hao, P., Duan, H., Zhao, W., Wang, Z., Yang, Z., and Li, X. (2023). Non-human primate models of focal cortical ischemia for neuronal replacement therapy. Journal of Cerebral Blood Flow & Metabolism *43*, 1456-1474.
Nath, T., Mathis, A., Chen, A.C., Patel, A., Bethge, M., and Mathis, M.W. (2019). Using DeepLabCut for 3D markerless pose estimation across species and behaviors. Nature protocols *14*, 2152-2176.
Nathan, P., and Smith, M.C. (1955). Long descending tracts in man: I. Review of present knowledge. Brain *78*, 248-303.
Nudo, R.J., and Milliken, G.W. (1996). Reorganization of movement representations in primary motor cortex following focal ischemic infarcts in adult squirrel monkeys. Journal of neurophysiology *75*, 2144-2149.
Nudo, R.J., Wise, B.M., SiFuentes, F., and Milliken, G.W. (1996). Neural substrates for the effects of rehabilitative training on motor recovery after ischemic infarct. Science *272*, 1791-1794.
Onodera, S., and Hicks, T.P. (2010). Carbocyanine dye usage in demarcating boundaries of the aged human red nucleus. PloS one *5*, e14430.
Porter, R. (1987). Corticomotoneuronal projections: synaptic events related to skilled movement. Proceedings of the Royal society of London. Series B. Biological sciences *231*, 147-168.
Porter, R., and Lemon, R.N. (1993). Corticospinal function and voluntary movement (Oxford University Press).
Ralston, D.D., Milroy, A.M., and Holstege, G. (1988). Ultrastructural evidence for direct monosynaptic rubrospinal connections to motoneurons in Macaca mulatta. Neuroscience letters *95*, 102-106.
Rathelot, J.-A., and Strick, P.L. (2006). Muscle representation in the macaque motor cortex: an anatomical perspective. Proceedings of the National Academy of Sciences *103*, 8257-8262.
Rathelot, J.-A., and Strick, P.L. (2009). Subdivisions of primary motor cortex based on cortico-motoneuronal cells. Proceedings of the National Academy of Sciences *106*, 918-923.
Riddle, C.N., Edgley, S.A., and Baker, S.N. (2009). Direct and indirect connections with upper limb motoneurons from the primate reticulospinal tract. Journal of Neuroscience *29*, 4993-4999.
Rouiller, E., Yu, X., Moret, V., Tempini, A., Wiesendanger, M., and Liang, F. (1998). Dexterity in adult monkeys following early lesion of the motor cortical hand area: the role of cortex adjacent to the lesion. European Journal of Neuroscience *10*, 729-740.
Shelton, F.D.N., and Reding, M.J. (2001). Effect of lesion location on upper limb motor recovery after stroke. Stroke *32*, 107-112.
Sukal, T.M., Ellis, M.D., and Dewald, J.P. (2007). Shoulder abduction-induced reductions in reaching work area following hemiparetic stroke: neuroscientific implications. Experimental brain research *183*, 215-223.
Takakusaki, K., Kohyama, J., Matsuyama, K., and Mori, S. (2001). Medullary reticulospinal tract mediating the generalized motor inhibition in cats: parallel inhibitory mechanisms acting on motoneurons and on interneuronal transmission in reflex pathways. Neuroscience *103*, 511-527.
Tapia, J.A., Tohyama, T., Poll, A., and Baker, S.N. (2022). The existence of the StartReact effect implies reticulospinal, not corticospinal, inputs dominate drive to motoneurons during voluntary movement. Journal of Neuroscience *42*, 7634-7647.
Ten Donkelaar, H. (1988). Evolution of the red nucleus and rubrospinal tract. Behavioural brain research *28*, 9-20.
Tower, S.S. (1940). Pyramidal lesion in the monkey. Brain *63*, 36-90.
Twitchell, T. (1951). The restoration of motor function following hemiplegia in man. Brain *74*, 443-480.
Van Kan, P.L., and McCurdy, M.L. (2001). Role of primate magnocellular red nucleus neurons in controlling hand preshaping during reaching to grasp. Journal of Neurophysiology *85*, 1461-1478.
Van Kan, P.L., and McCurdy, M.L. (2002a). Contribution of primate magnocellular red nucleus to timing of hand preshaping during reaching to grasp. Journal of neurophysiology *87*, 1473-1487.
Van Kan, P.L., and McCurdy, M.L. (2002b). Discharge of primate magnocellular red nucleus neurons during reaching to grasp in different spatial locations. Experimental brain research *142*, 151-157.

Walshe, F. (1961). The problem of the origin of the pyramidal tract. Scientific aspects of neurology. Edinburgh: ES Livingstone.
Ward, N., Brown, M., Thompson, A., and Frackowiak, R. (2003). Neural correlates of outcome after stroke: a cross-sectional fMRI study. Brain *126*, 1430-1448.
Widener, G.L., and Cheney, P.D. (1997). Effects on muscle activity from microstimuli applied to somatosensory and motor cortex during voluntary movement in the monkey. Journal of neurophysiology *77*, 2446-2465.
Witham, C.L., Fisher, K.M., Edgley, S.A., and Baker, S.N. (2016). Corticospinal inputs to primate motoneurons innervating the forelimb from two divisions of primary motor cortex and area 3a. Journal of neuroscience *36*, 2605-2616.
Zaaimi, B., Edgley, S.A., Soteropoulos, D.S., and Baker, S.N. (2012). Changes in descending motor pathway connectivity after corticospinal tract lesion in macaque monkey. Brain *135*, 2277-2289.
Zaaimi, B., Soteropoulos, D.S., Fisher, K.M., Riddle, C.N., and Baker, S.N. (2018). Classification of neurons in the primate reticular formation and changes after recovery from pyramidal tract lesion. Journal of Neuroscience *38*, 6190-6206.

Figures and Legends

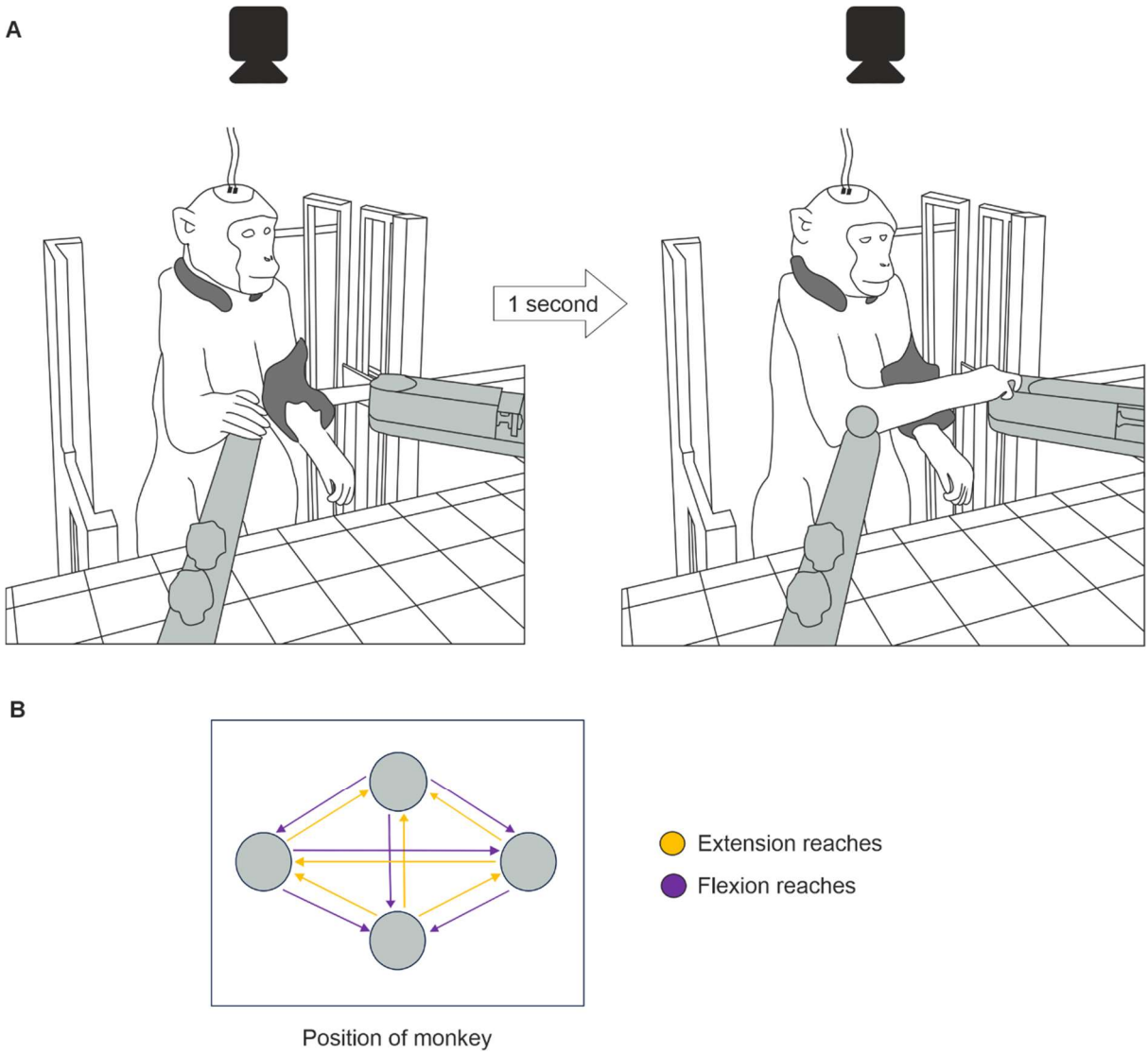

Figure 1. Behavioral Task. A, drawings of the reaching task setup. Monkeys were placed in a neck and left arm restraint (dark grey). Handle and cup (light grey) positions were fixed to the table; here the trial has the handle on the animal's right, and the cup on the left. Holding the handle for one second unlocked the cup, and the food reward was retrieved. A camera positioned above the monkey recorded high speed video footage. EMG was recorded from implanted wires via connectors on the headpiece (not used in this report). B, twelve possible handle and cup arrangements for assessing both extension and flexion reach performance, shown with the same perspective as the camera's field of view.

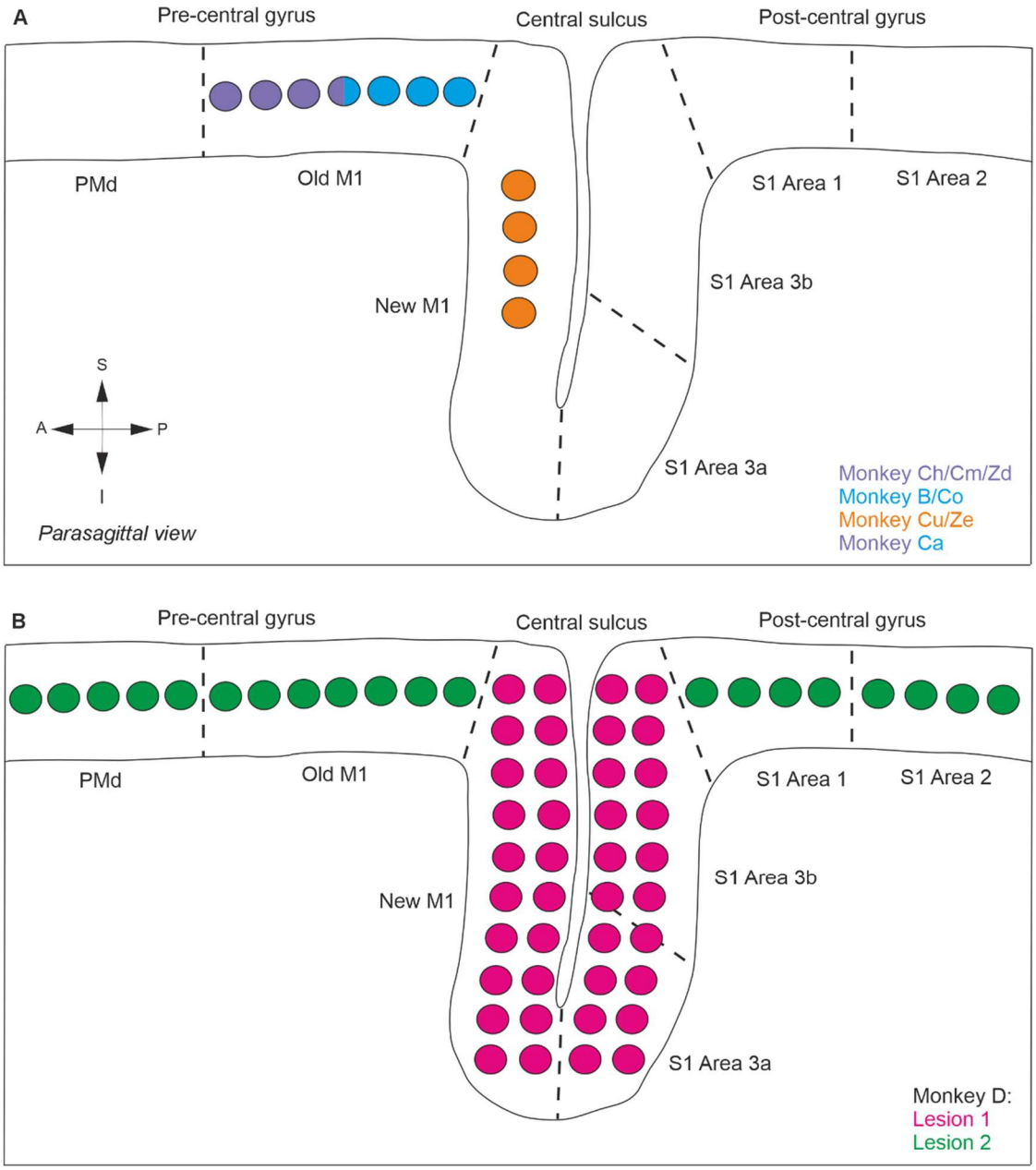

Figure 2. Lesion Locations. A, diagram showing anteroposterior extent of focal lesions performed in different regions of M1. Each circle represents a needle injection site at a single laterality, which extended in a grid 8-19 mm lateral from midline for all animals. Anterior Old M1 lesion (purple); Posterior Old M1 lesion (blue); Entire Old M1 (purple and blue); New M1 lesion (orange). B, diagram of lesion sites performed in Monkey D during two surgeries. Deeper lesions of anterior and posterior banks of the central sulcus (pink); superficial lesions of PMd, Old M1, S1 Brodmann's Areas 1 and 2 (green).

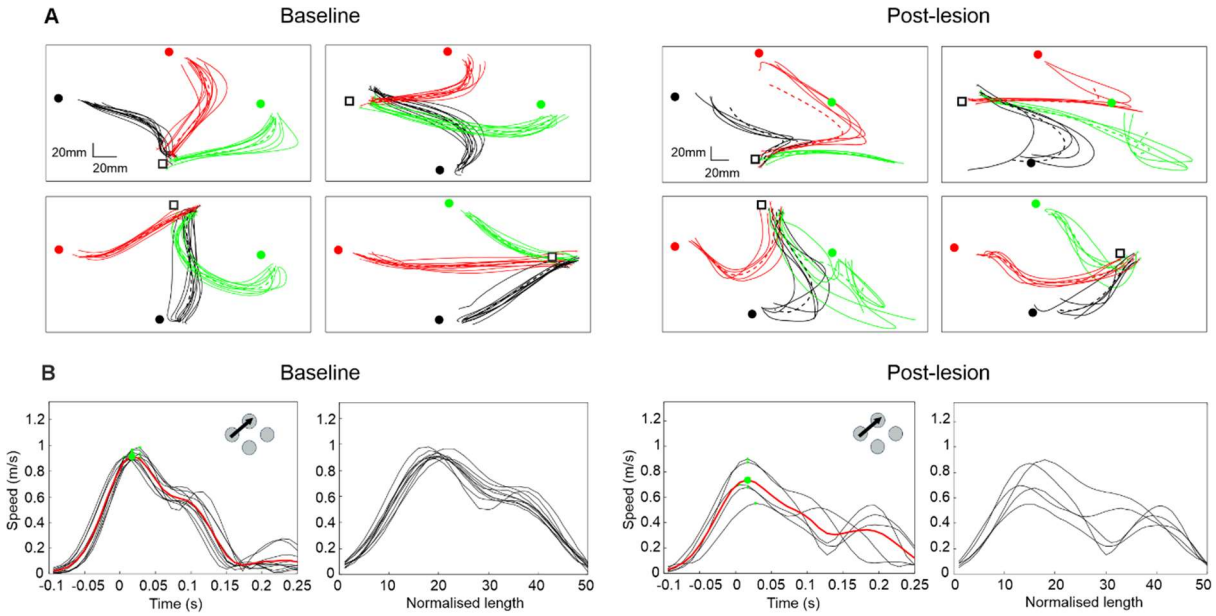

Figure 3. Example Kinematics. A, reach trajectories plotted from DeepLabCut predictions of hand location converted to physical distance (mm). Results are from Monkey D (New M1 and S1 Brodmann's Area 3a/b lesion), demonstrating an example baseline session (left four plots) and early post-lesion session (right four plots). Each plot represents a different handle (start of reach, black square) location, with three corresponding cup (end of reach; black, red or green circles) positions. Repeats of the same reaching movement are overlaid in the same color. Dotted lines show mean trajectories. B, hand speed plotted for all trials for one movement direction, shown from same baseline and post-lesion sessions as in (A). The left most plot for each session represents hand speed plotted 0.1 s before to 0.25 s after handle release (time 0 s). Green dots, maximum speeds per trial; red trace, mean speed over all trial repeats. The right most plots display overlaid speed traces, normalized to last 50-samples from when the hand first exceeds (reach start) and then returns below (reach end) 0.1 m/s.

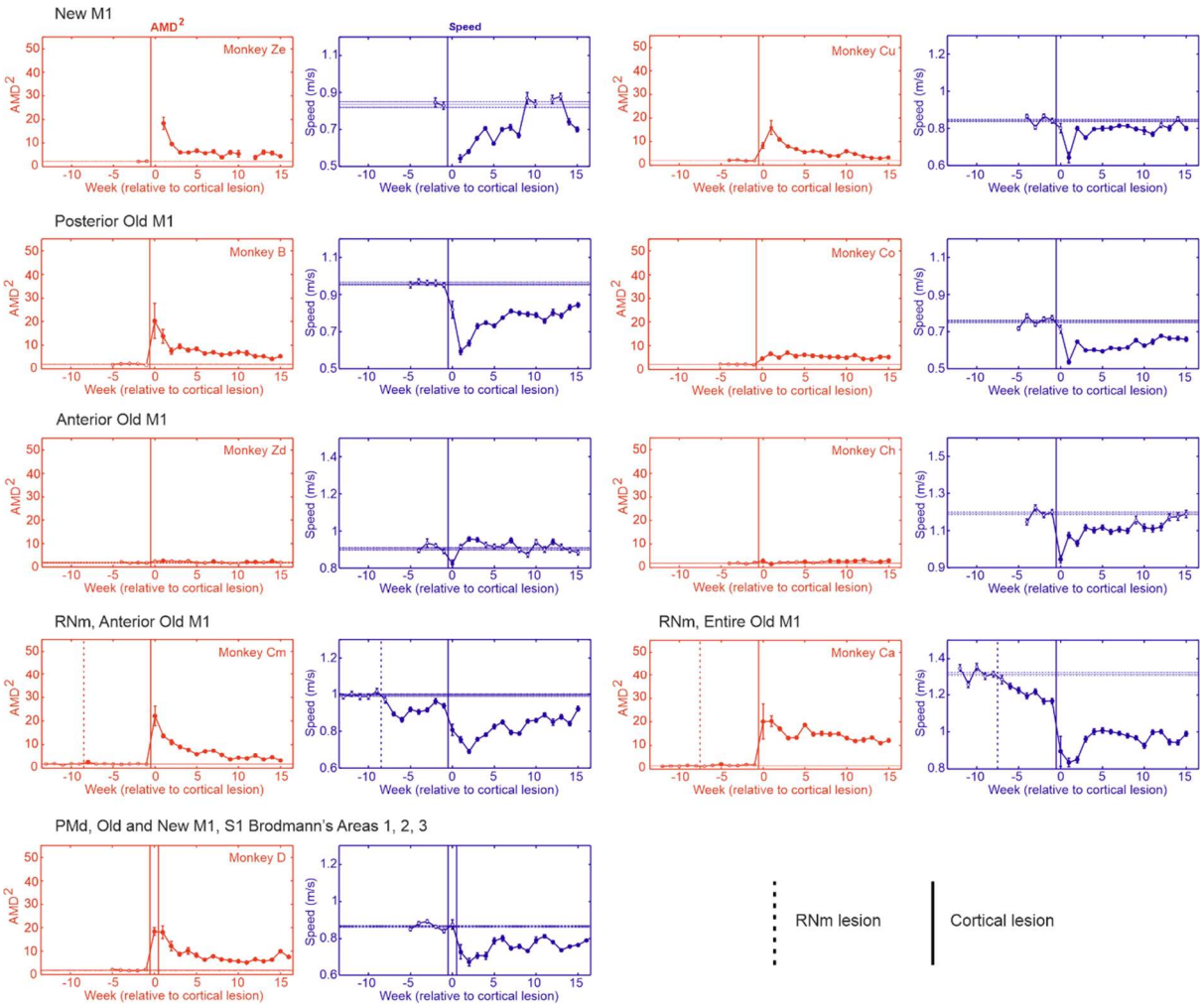

Figure 4. Maximum Speed and Trajectory Variability per Week Averaged Over All Reaching Directions. Each row relates to a different lesion site. Red graphs show average Mahalanobis distance squared (AMD^2) per week; blue graphs show average maximum speed per week; vertical lines show lesion times (RNm or cortical); horizontal lines indicate baseline mean ± standard error. Range of the AMD^2 and speed axes are the same across all plots to allow easier visual comparison. For AMD^2 graphs (red), circles are median values from all trials performed that week. Standard error of the median was calculated by bootstrapping with 1000 iterations (error bars). For speed graphs (blue), circles represent mean weekly values, error bars show standard error of mean. Filled circles are significantly different from baseline ($p < 0.05$), identified using the two-sample t test and corrected for multiple comparisons using the Benjamini-Hochberg procedure with a false discovery rate of 5%.

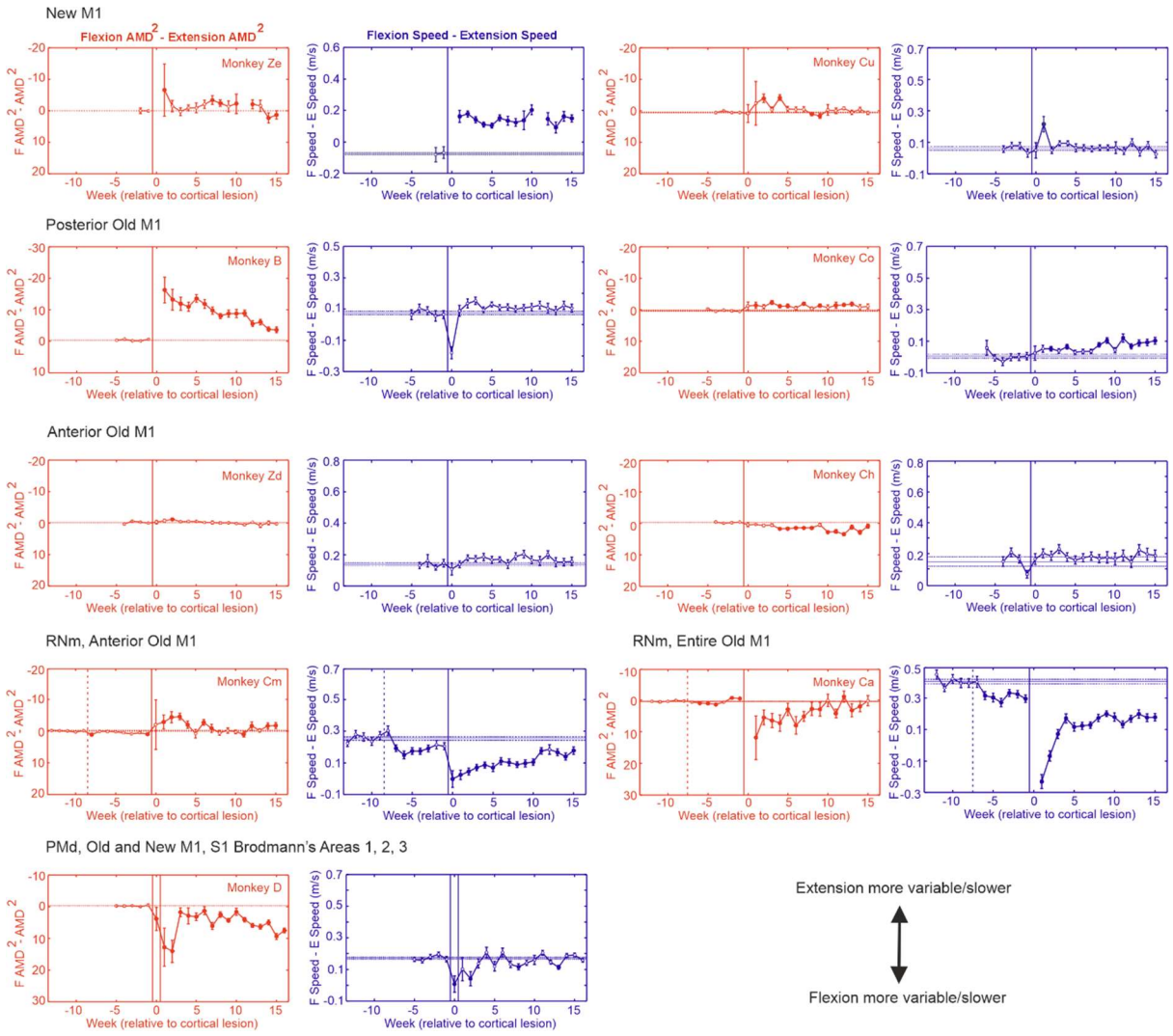

Figure 5. Maximum Speed and Trajectory Variability per Week, Compared for Flexion vs Extension Reaching Directions. Similar display as Fig. 4, but results shown are the difference between flexion and extension values to appreciate any differences. Y axis scale range is comparable across all plots of the same type between monkeys to allow easier visual comparison. Note that the axis scale has been inverted for AMD^2, so that worse performance in extension is shown by upwards deflection for both AMD^2 and speed.

Lesion Region(s)	Trajectory Variability	Speed	Directional Bias of Impairment	Flexor Synergy
New M1	+++	++	Extension	-
Posterior Old M1	++	+++	Extension	-
Anterior Old M1	+	+	-	-
RNm, Anterior Old M1	++	+++	Flexion	-
RNm, Entire Old M1	+++	++++	Flexion	-
PMd, M1, S1 Brodmann's Areas 1, 2 and 3	+++	++	Flexion	-

Table 1. Summary of the Lesion Impacts on Assessments of Reaching Performance.